

proteins suggest that such a universal inhibitor design could potentially be effective against several different viruses.^[18]

Received: July 16, 2001 [Z17509]

A Breathing Hybrid Organic–Inorganic Solid with Very Large Pores and High Magnetic Characteristics

Karin Barthelet, Jérôme Marrot, Didier Riou,* and Gérard Férey

Porous solids^[1] usually find applications in the areas of ion-exchange, separation, and catalysis. The recent discovery of new materials based upon transition metal ions^[2] opens the possibility of making open frameworks that exhibit also some of the remarkable electronic properties of condensed transition metal compounds (ferro- and ferrimagnetism, metal-semiconductor transitions, ferroelectricity, combined ionic/electrical conductivity). Up to now, in the field of magnetism, the major limitation for producing porous solids with high ordering temperatures came from the structure itself. Indeed, most of the porous compounds are built from metallic clusters linked by diamagnetic linkers (phosphates, arsenates, silicates, aliphatic chains) which prevent strong, long-range interactions. To date, the highest Néel temperatures were observed for the purely inorganic porous skeleton of ULM-3^[3] (37 K) and for the hybrid solid HKUST-1^[4] (75 K).

To overcome this difficulty, our design strategy is to link chains of corner-sharing transition metal octahedra (which favor strong, long-range superexchange coupling) by rigid organic linkers containing delocalized π electrons for the three-dimensional transmission of the interactions. The use of such linkers was mainly developed by the groups of Yaghi and O'Keeffe,^[5a] Zaworotko,^[5b] and Kitagawa^[5c] for metal-organic frameworks with modulable very large pores.

As an example of our design principle, we describe here the synthesis, structure, magnetic and sorption properties of a large-pore, flexible, open framework (MIL-47) that is antiferromagnetic below 95 K.

To implement this design, we used the hydrothermal reaction (teflon-lined steel autoclave Parr, four days, 473 K, autogenous pressure, filling rate: 50 %) of either a mixture of VCl_3 , terephthalic acid, and desionized water (molar ratio 1:0.25:100), which only provides homogeneous pure powders, or of vanadium metal, terephthalic acid, hydrofluorhydric acid, and water (molar ratio 1:0.25:2:250) when crystals are needed. In both cases, the pH value remains 1 throughout the synthesis and the yield is close to 15 %. The resulting light yellow product, (hereafter labeled MIL-47as), which is stable in air, is formulated $\text{V}^{\text{III}}(\text{OH})\{\text{O}_2\text{C}-\text{C}_6\text{H}_4-\text{CO}_2\} \cdot x(\text{HO}_2\text{C}-\text{C}_6\text{H}_4-\text{CO}_2\text{H})$ ($x \sim 0.75$) on the basis of elemental analysis (calcd: C 47.1, V 14.3; found: C 46.87, V 13.79;). Both thermogravimetry and thermal analyses (TGA2050 TA apparatus, O_2 flow, heating rate 2 K min^{-1}) show (Figure 1a) a decomposition of MIL-47as in two steps between 300 and 420°C . The first weight loss (exp.: 32.3 %, calcd: 34.92 % for

- [1] For a recent review, see A. G. Cochran, *Chem. Biol.* **2000**, 7, R85–R94.
- [2] a) A. Degterev, A. Lugovskoy, M. Cardone, B. Mulley, G. Wagner, T. Mitchison, J. Yuan, *Nat. Cell. Biol.* **2001**, 3, 173–182; b) A. K. Debnath, L. Radigan, S. Jiang, *J. Med. Chem.* **1999**, 42, 3203–3209; c) S. A. Qureshi, R. M. Kim, Z. Konteatis, D. E. Biazzo, H. Motamedi, R. Rodrigues, J. A. Boice, J. R. Calaycay, M. A. Bednarek, P. Griffin, Y.-D. Gao, K. Chapman, D. F. Mark, *Proc. Natl. Acad. Sci. USA* **1999**, 96, 12156–12161; d) S.-S. Tian, P. Lamb, A. G. King, S. G. Miller, L. Kessler, J. I. Luengo, L. Averill, R. K. Johnson, J. G. Gleason, L. M. Pelus, S. B. Dillon, J. Rosen, *Science* **1998**, 281, 257–259; e) J. W. Tilley, L. Chen, D. C. Fry, S. D. Emerson, G. D. Powers, D. Biondi, T. Varnell, R. Trilles, R. Guthrie, F. Mennona, G. Kaplan, R. A. LeMahieu, M. Carson, R. Han, C.-M. Liu, R. Palermo, G. Ju, *J. Am. Chem. Soc.* **1997**, 119, 7589–7590.
- [3] a) D. C. Chan, D. Fass, J. M. Berger, P. S. Kim, *Cell* **1997**, 89, 263–273; b) M. Lu, P. S. Kim, *J. Bio. Mol. Struct. Dyn.* **1997**, 15, 465–471.
- [4] For a review, see D. C. Chan, P. S. Kim, *Cell* **1998**, 93, 681–684.
- [5] a) M. Lu, S. C. Blacklow, P. S. Kim, *Nat. Struct. Biol.* **1995**, 2, 1075–1082; b) M. Ferrer, T. M. Kapoor, T. Strassmaier, W. Weissenhorn, J. J. Skehel, D. Oprian, S. L. Schreiber, D. C. Wiley, S. C. Harrison, *Nat. Struct. Biol.* **1999**, 6, 953–960.
- [6] a) S. Jiang, K. Lin, N. Strick, A. Neurath, *Nature* **1993**, 365, 113; b) C. T. Wild, D. C. Shugars, T. K. Greenwell, C. B. McDaniel, T. J. Matthews, *Proc. Natl. Acad. Sci. USA* **1994**, 91, 9770–9774.
- [7] a) R. A. Furuta, C. T. Wild, Y. Weng, C. D. Weiss, *Nat. Struct. Biol.* **1998**, 5, 276–279; b) J. M. Kilby, S. Hopkins, T. M. Venetta, B. DiMassimo, G. A. Cloud, J. Y. Lee, L. Alldredge, E. Hunter, D. Lambert, D. Bolognesi, T. Matthews, M. R. Johnson, M. A. Nowak, G. M. Shaw, M. S. Saag, *Nat. Med.* **1998**, 4, 1302–1307.
- [8] D. M. Eckert, V. N. Malashkevich, L. H. Hong, P. A. Carr, P. S. Kim, *Cell* **1999**, 99, 103–115.
- [9] S. Jiang, A. K. Debnath, *Biochem. Biophys. Res. Commun.* **2000**, 269, 641–646.
- [10] D. C. Chan, C. T. Chutkowski, P. S. Kim, *Proc. Natl. Acad. Sci. USA* **1998**, 95, 15613–15617.
- [11] J. K. Judice, J. Y. K. Tom, W. Huang, T. Wrin, J. Vennari, C. J. Petropoulos, R. S. McDowell, *Proc. Natl. Acad. Sci. USA* **1997**, 94, 13426–13430.
- [12] S. Jiang, K. Lin, *Peptide Res.* **1995**, 8, 345–348.
- [13] B. P. Orner, J. T. Ernst, A. D. Hamilton, *J. Am. Chem. Soc.* **2001**, 123, 5382–5383.
- [14] K. Mislow, M. A. Glass, R. E. O'Brien, P. Rutkin, D. Steinberg, J. Weiss, C. Djerassi, *J. Am. Chem. Soc.* **1962**, 84, 1455–1478.
- [15] See Supporting Information.
- [16] a) S. Jiang, K. Lin, L. Zhang, A. K. Debnath, *J. Virol. Methods* **1999**, 80, 85–96; b) S. Jiang, K. Lin, M. Lu, *J. Virol.* **1998**, 72, 10213–10217.
- [17] S. Jiang, K. Lin, N. Strick, A. R. Neurath, *Biochem. Biophys. Res. Commun.* **1993**, 195, 533–538.
- [18] a) For a review, see J. J. Skehel, D. C. Wiley, *Cell* **1998**, 95, 871–874; b) P. A. Bullough, F. M. Hughson, J. J. Skehel, D. C. Wiley, *Nature* **1994**, 371, 37–43; c) C. M. Carr, P. S. Kim, *Cell* **1993**, 73, 823–832; d) D. Fass, S. C. Harrison, P. S. Kim, *Nat. Struct. Biol.* **1996**, 3, 465–469; e) V. N. Malashkevich, D. C. Chan, C. T. Chutkowski, P. S. Kim, *Proc. Natl. Acad. Sci. USA* **1998**, 95, 9134–9139; f) M. Caffrey, M. Cai, J. Kaufman, S. J. Stahl, P. T. Wingfield, D. G. Covell, A. M. Gronenborn, G. M. Clore, *EMBO* **1998**, 17, 4572–4584.

[*] Prof. Dr. D. Riou, K. Barthelet, Dr. J. Marrot, Prof. Dr. G. Férey
 Institut Lavoisier UMR CNRS 8637
 Université de Versailles
 St Quentin en Yvelines
 45 Avenue des Etats-Unis, 78035 Versailles Cedex (France)
 Fax: (+33)1-3925-4358
 E-mail: riou@chimie.uvsq.fr

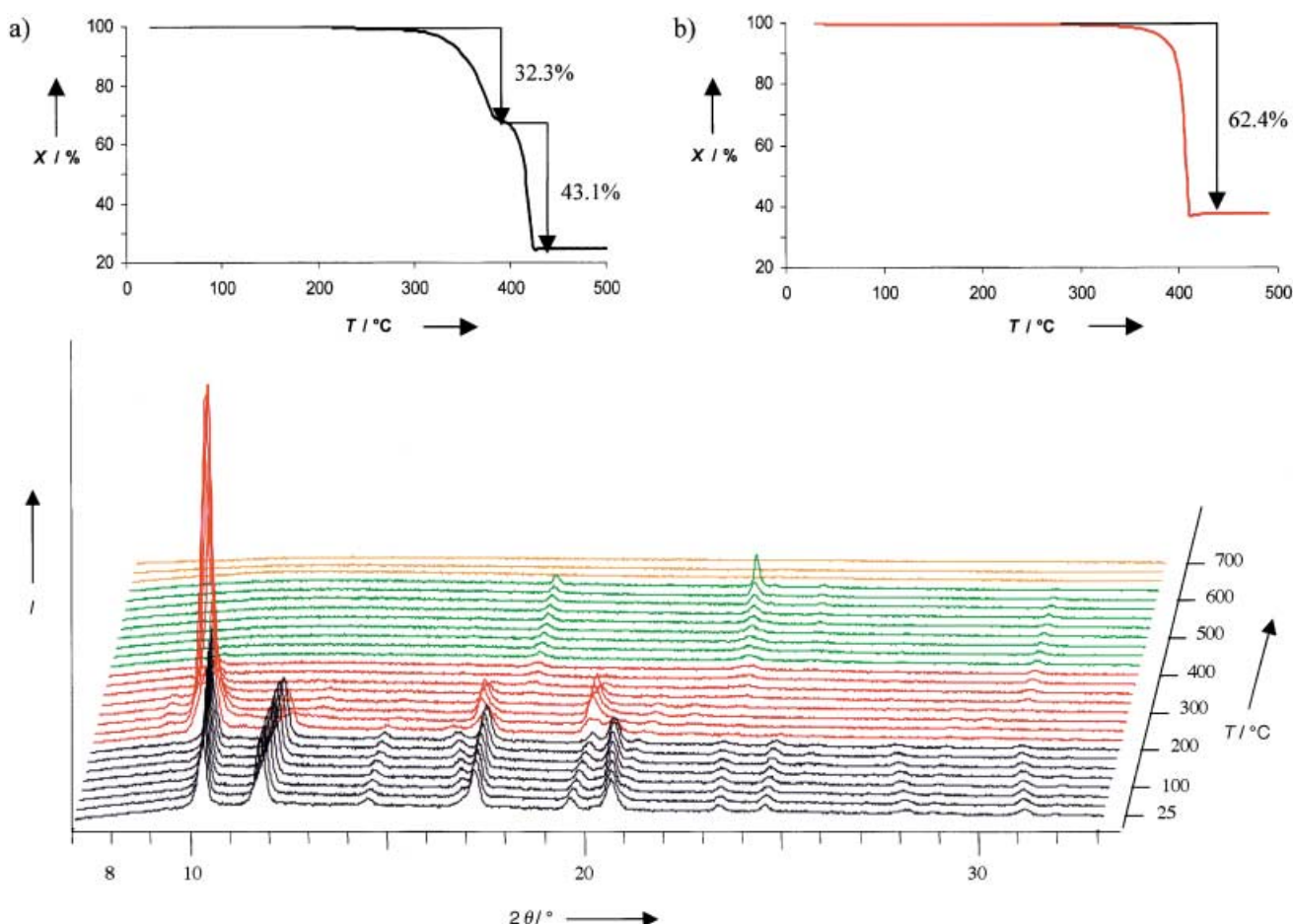


Figure 1. Thermogravimetric analysis of MIL-47as, showing the two steps of transformation. Inserts a) and b) give the thermogravimetric curves of MIL-47as and MIL-47, respectively.

$x = 0.75$) represents the evacuation of the terephthalic acid guest to produce the evacuated $V^{IV}O\{O_2C-C_6H_4-CO_2\}$ (hereafter MIL-47) (vide infra). The second step (exp.: 43.1%, calcd: 40.30% for $x = 0.75$) relates to combustion of the terephthalic acid of the framework. The residue is a mixture of VO_2 and V_2O_5 . Evacuated MIL-47 can be obtained pure by calcination (for 250 mg) 24 h under air at 573 K in a tubular furnace. MIL-47 decomposes at 673 K in one step (Figure 1 b). The experimental X-ray patterns are in excellent agreement with those calculated from single-crystal data.

Single crystals of both MIL-47as and MIL-47 were examined by X-ray diffraction.^[6] Both solids present the same topology with a three-dimensional orthorhombic structure that exhibits large pores (free diameter taking account the Van der Waals radii: 7.9×12.0 Å for MIL-47as and 10.5×11.0 Å for MIL-47) in the [100] direction (Figure 2). Each tunnel is delimited by four walls of benzyl units and four chains of corner-shared vanadium octahedra (Figure 2). As shown by valence bond calculations^[7] the shared vertices are hydroxy groups associated with V^{III} in MIL-47as and oxygen atoms associated with V^{IV} in MIL-47. The six V–O distances lie in the range $1.946(2) - 1.998(2)$ Å, which is usual for V^{III} –O bonds, for MIL-47as. In MIL-47, along the chains, the alternation of short (1.672 Å) and long (2.102 Å) bonds is typical of V^{IV} in octahedral coordination. In MIL-47as, the terephthalic acid guest is highly disordered. Although its

refinement was not possible, chemical analysis, density measurements (exp.: 1.597(8); calcd: 1.613, Micromeritics multipycnometer), and the recrystallization of terephthalic acid in the cold parts of the apparatus during the degassing phase of MIL-47as for BET measurements confirm the hypothesis. The carboxylate groups of the framework terephthalate link two adjacent octahedra of one chain. The resulting strong tilting of the octahedra leads to a V–O–V superexchange angle of $124.0(2)^\circ$ for MIL-47as and of 129.38° for MIL-47. Such a topology is close to that of $[(CuSiF_6(4,4'-bipyridine)_2)_n]$ previously described by Kitagawa et al.^[5c] in which the chains are formed by alternation of CuN_2F_4 and SiF_6 octahedra linked by corners, leading to two-dimensional (2D) magnetic behavior.

At room temperature, the crystallinity of MIL-47 is preserved; density (calcd: 1.00) and thermogravimetric analysis (TGA) measurements indicate that it does not reabsorb atmospheric water. The permanent porosity of the evacuated MIL-47 was confirmed by gas sorption isotherm experiments performed (Micromeritics ASAP2010) in liquid nitrogen. While MIL-47as evidently does not present any capacity for N_2 sorption, MIL-47 reveals a type I isotherm (Figure 3) without hysteresis upon desorption. The measured BET surface area is $930(30) \text{ m}^2 \text{ g}^{-1}$ and, assuming monolayer coverage by N_2 , the Langmuir surface area is estimated to be $1320(2) \text{ m}^2 \text{ g}^{-1}$.

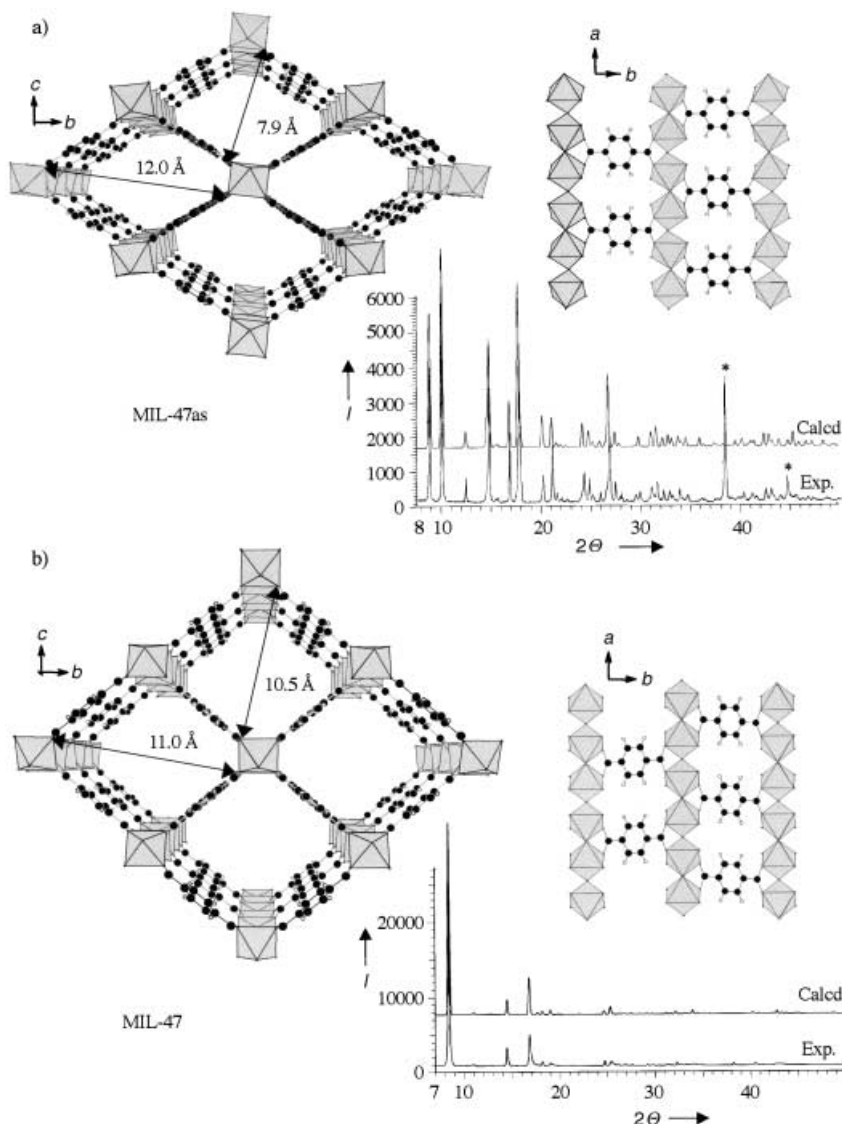


Figure 2. Projections of the structures of MIL-47as (a) and of MIL-47 (b), and X-ray powder patterns (experimental and calculated) of the two phases. Guest atoms in MIL-47as are omitted for clarity (* peaks of the aluminum sample holder).

The noticeable flexibility of the framework with and without guest, deduced from the structure determinations, is easily evidenced by the evolution of the X-ray powder pattern (Figure 2) between the filled and evacuated phases. This

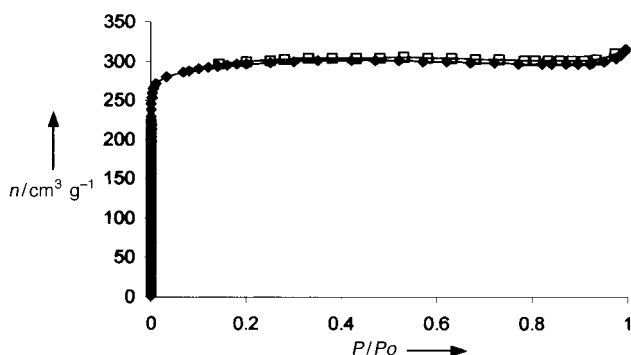


Figure 3. N₂ sorption and desorption isotherms measured at 77 K for MIL-47 (♦ = sorption, □ = desorption; P₀ = 1 atm).

allows us to monitor the desorption–adsorption of gases by evacuated MIL-47 by X-ray diffraction at room temperature. For instance, the readsorption of diethyl ether is achieved after 72 h. Guest exchange studies also show that the structural integrity of the framework is maintained in solution without any loss of crystallinity. Typically, introduction of MIL-47 in trimethylbenzene and 2-methyl-1-propanol gives the MIL-47as framework after reaction times that are dependent on the nature of the liquid, but which do not exceed 72 h.

Magnetic measurements performed on MIL-47as indicate (Figure 4) antiferromagnetic behavior below $T_N = 95(5)$ K. The fit of the paramagnetic part of the $1/\chi$ curve between 180 and 300 K with a Curie–Weiss law provides a paramagnetic temperature θ_p of $-186(4)$ K, indicative of strong antiferromagnetic interactions. The Curie constant of $1.04(2)$ is typical of V^{3+} ions (theoretical value 1). According to Goodenough rules,^[8] $V^{3+} - V^{3+}$ interactions are predicted to be ferromagnetic if the superexchange angle is close to 180° , with vanadium in an octahedral coordination site but the sign of the exchange integral J can be inverted when the V–O–V angle decreases below the so-called “blank angle”. It is probably the case here, since the superexchange angle is only 124° , due to the effect of chelation by carboxylates between two octahedra. It is likely that this low value corresponds to antiferromagnetic interactions within and between chains. Otherwise, if 124° is larger than the blank angle, the magnetic structure would correspond to the antiferromagnetic coupling of ferromagnetic chains. The same behavior is observed with MIL-47 with a lower T_N ($75(5)$ K) value, which is related to the weaker $V^{4+} - V^{4+}$ ($d^1 - d^1$) interactions. However, the

striking feature that confirms our strategy is the drastic effect of π electrons on the temperature of magnetic ordering. Other structures, built with the same chains of V^{4+} ions with similar superexchange angles and interchain distances,^[9] but without

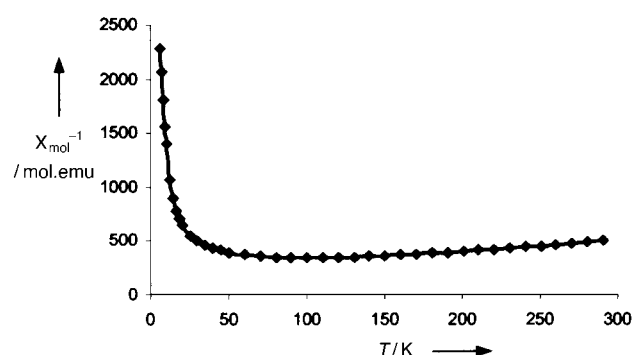


Figure 4. Reciprocal molar magnetic susceptibility as a function of the temperature for MIL-47as.

delocalized electrons on the linkers between the chains, exhibit very low T_N values (4–10 K). The presence of these π electrons drastically enhances the magnetic characteristics of these solids above the strategic borderline of liquid nitrogen temperature. This renders porous solids magnetic with sufficiently high and available ordering temperatures which could now find applications, for example, in magnetic sorting.

Received: August 1, 2001 [Z17651]

- [1] A. K. Cheetham, G. Férey, T. Loiseau, *Angew. Chem.* **1999**, *111*, 3466–3492; *Angew. Chem. Int. Ed.* **1999**, *38*, 3268–3292.
- [2] M. Cavellec, D. Riou, C. Ninclaus, J. M. Grenèche, G. Férey, *Zeolites* **1996**, *17*, 260; M. Cavellec, D. Riou, G. Férey, *Inorg. Chem. Acta* **1999**, *291*, 317; K.-H. Lii, Y.-F. Huang, V. Zima, C.-Y. Huang, H.-M. Lin, Y.-C. Jiang, F.-L. Liao, S.-L. Wang, *Chem. Mater.* **1998**, *10*, 2599.
- [3] M. Cavellec, D. Riou, J. M. Grenèche, G. Férey, *J. Magn. Mater.* **1996**, *163*, 173.
- [4] X. X. Zhang, S. S.-Y. Chui, I. D. Williams, *J. Appl. Phys.* **2000**, *87*, 6007–6009.
- [5] a) H. Li, M. Eddaoudi, M. O’Keeffe, O. M. Yaghi, *Nature* **1999**, *402*, 276; B. L. Chen, M. Eddaoudi, S. T. Hyde, M. O’Keeffe, O. M. Yaghi, *Science* **2001**, *291*, 1021; b) S. A. Bourne, J. Lu, A. Mondal, B. Moulton, M. J. Zaworotko, *Angew. Chem.* **2001**, *113*, 2171–2174; *Angew. Chem. Int. Ed.* **2001**, *40*, 2111–2113; J. Lu, A. Mondal, B. Moulton, M. J. Zaworotko, *Angew. Chem.* **2001**, *113*, 2169–2174; *Angew. Chem. Int. Ed.* **2001**, *40*, 2113–2116; c) S.-I. Noro, S. Kitagawa, M. Kondo, K. Seki, *Angew. Chem.* **2000**, *112*, 2161–2164; *Angew. Chem. Int. Ed.* **2000**, *39*, 2081–2084; d) S. S. Y. Chui, S. M.-F. Lo, J. P. H. Charmant, A. G. Orpen, I. D. Williams, *Science* **1999**, *283*, 1148.
- [6] Crystal structure analysis of MIL-47as: crystal dimensions: $0.140 \times 0.120 \times 0.020$ mm; orthorhombic; space group *Pnma* (no 62); $a = 17.519(1)$, $b = 6.8750(4)$, $c = 12.1680(8)$ Å, $V = 1465.5(2)$ Å³; $Z = 4$; reflections collected: 9709; independent reflections: 2144; $R(\text{int}) = 0.1053$; a hemisphere of data was collected up to $2\theta \approx 60^\circ$; an empirical absorption correction was applied (SADABS) ($\mu = 7.17 \text{ cm}^{-1}$; min/max transmission 0.9063/0.9858); 119 parameters; $R1(F_o) = 0.0694$, $wR2(F_o^2) = 0.1345$ for 2144 unique reflections $I \geq 2\sigma(I)$; highest positive and negative residual electron density 0.495/–0.451 e Å^{–3}. Crystal structure analysis of MIL-47: crystal dimensions: $0.100 \times 0.080 \times 0.060$ mm; orthorhombic; space group *Pnma* (no 62); $a = 6.818(1)$, $b = 16.143(3)$, $c = 13.939(2)$ Å, $V = 1534.1(5)$ Å³; $Z = 4$; reflections collected: 6596; independent reflections: 1160; $R(\text{int}) = 0.2774$; a hemisphere of data was collected up to $2\theta \approx 60^\circ$; an empirical absorption correction was applied (SADABS) ($\mu = 6.41 \text{ cm}^{-1}$; min/max transmission 0.9387/0.9626); 68 parameters; $R1(F_o) = 0.0766$, $wR2(F_o^2) = 0.1098$ for 1160 unique reflections $I \geq 2\sigma(I)$; highest positive and negative residual electron density 0.455/–0.483 e Å^{–3}. For both compounds, the data were collected at room temperature with a Siemens SMART three-circle diffractometer equipped with a CCD bidimensionnal detector and working with $\text{MoK}\alpha$ ($\lambda = 0.71073$ Å) monochromatized radiation. An empirical absorption correction was applied by using the SADABS program based on Blessing’s method.^[10] The structure solutions were determined by direct methods then refined with the SHELX-TL package.^[11] The hydrogen atoms of the aromatic cycles were located by applying geometrical constraints. The structures were generated with the DIAMOND program (K. Brandenburg, Crystal Impact GbR, **1999**). Crystallographic data (excluding structure factors) for the structures reported in this paper have been deposited with the Cambridge Crystallographic Data Centre as supplementary publication no. CCDC-166784 (MIL-47as) and CCDC-166785 (MIL-47). Copies of the data can be obtained free of charge on application to CCDC, 12 Union Road, Cambridge CB21EZ, UK (fax: (+44) 1223-336-033; e-mail: deposit@ccdc.cam.ac.uk).
- [7] N. E. Brese, M. O’Keeffe, *Acta Crystallogr. Sect. B* **1992**, *47*, 192.
- [8] J. B. Goodenough in *Magnetism and the Chemical Bond*, Interscience, New York, **1963**.
- [9] K. Barthelet, C. Jouve, D. Riou, G. Férey, *Solid State Sciences* **2000**, *2*, 871.

- [10] a) R. Blessing, *Acta Crystallogr. Sect. A* **1995**, *51*, 33; b) G. M. Sheldrick, a program for the Siemens Area Detector Absorption Correction, University of Göttingen, Germany, **1997**.
- [11] G. M. Sheldrick, SHELX-TL version 5.03, Software Package for the Crystal Structure Determination Siemens Analytical X-ray Instruments Inc., Madison, Wisconsin, USA **1994**.

Infinite Secondary Building Units and Forbidden Catenation in Metal-Organic Frameworks**

Nathaniel L. Rosi, Mohamed Eddaoudi, Jaheon Kim, Michael O’Keeffe, and Omar M. Yaghi*

Catenation, in the form of interpenetrating and interweaving,^[1] has been a major concern in the design of low-density (porous) structures due to the following widely held beliefs: a) the use of long links for the design of frameworks with large pores results in catenated structures and thus small pores, b) highly catenated frameworks typically have low porosity (<20%), and c) catenation contributes negatively to the structural stability and porosity of open frameworks.^[1, 2] We recently found in the chemistry of metal-organic frameworks (MOFs) that *discrete* secondary building units (SBUs) are important for designing structures with attributes that disprove the universality of b) and c); specifically, maximally interpenetrating MOFs have been shown to have highly porous (>65%) structures, and interweaving in open frameworks has been recognized and used for the design of structures with reinforced walls and permanent porosity.^[1c–d, 3]

Herein, we introduce the use of *infinite* SBUs toward addressing the point presented in a). Specifically, we show that MOF-69A, $[\text{Zn}_3(\text{OH})_2(\text{bpdc})_2] \cdot 4\text{DEF} \cdot 2\text{H}_2\text{O}$ (bpdc = 4,4'-biphenyldicarboxylate; DEF = *N,N'*-diethylformamide), and its 2,6-naphthalenedicarboxylate (ndc) analogue MOF-69B have three-dimensional (3D) structures constructed from infinite Zn-O-C SBUs and long bpdc or ndc links that expand the Al net in SrAl_2 and provide a framework where catenation is forbidden.

Infinite Zn-O-C SBUs were produced by subjecting reaction mixtures that typically give MOF-5 to increasing amounts of H_2O_2 .^[4] These solutions were monitored for the appearance of crystalline solids. A single-crystal X-ray diffraction study^[5a] performed on a rodlike colorless crystal of MOF-69A

[*] Prof. O. M. Yaghi, N. L. Rosi, Dr. M. Eddaoudi, Dr. J. Kim
Materials Design and Discovery Group
Department of Chemistry
University of Michigan
Ann Arbor, MI 48109-1055 (USA)
Fax: (+1) 734-615-9751
E-mail: oyaghi@umich.edu
Prof. M. O’Keeffe
Department of Chemistry and Biochemistry
Arizona State University
Tempe, AZ 85287-1604 (USA)

[**] The National Science Foundation support to M.O’K. (DMR-9804817) and O.M.Y. (DMR-9980469) is gratefully acknowledged.